Optimal Planning and Operation of Static VAR Compensators in a Distribution System with Non-linear Loads

Alvarez Alvarado, Manuel; Rodríguez-Gallegos , Carlos; Jayaweera, Dilan

Optimal Planning and Operation of Static VAR Compensators in a Distribution System with Non-linear Loads

Manuel S. Alvarez-Alvarado [1*], Carlos D. Rodríguez-Gallegos [2], Dilan Jayaweera [3]

[1,3] Department of Electronics, Electrical and Systems Engineering, University of Birmingham, Birmingham B15 2TT, Birmingham, United Kingdom
[2] Solar Energy Research Institute of Singapore, National University of Singapore, Singapore 117574, Singapore city, Singapore
[*] manuel.alvarez.alvarado@ieee.org

Abstract: This paper presents an innovative design for the optimal sizing, placement, and dispatch approach of Distribution Static Var Compensators (D-SVCs) in a radial power distribution system to improve the technical and economic aspects of the grid. The approach incorporates the Total Harmonic Distortion (THD) effects into the assessment with the presence of non-linear loads. A Multi Particle Swarm Optimization (MPSO) algorithm is also proposed, at first to select the placement and size and then to select the dispatch strategy of D-SVCs. Three IEEE test systems were used for the case study to show the efficacy of the method. The results reveal that the approach is viable and it determines the cases where the highest savings were achievable fulfilling the grid voltage and THD constraints.

1. Introduction

With the increase in population and rapid growth in industry and other sectors, the demand for the electricity raises [1]. This may not be necessarily managed by the addition of conventional and new generators unless intermediate mechanisms are in place in order to reduce grid electrical power losses and assure grid power quality, efficiency, and other operational benefits.

Furthermore, power electronic devices are typically employed to enable loads to operate with high capacity, high performance and low cost [2]. Nevertheless, they present a drawback as these devices are commonly represented by non-linear loads, which affect the grid quality and increment the electrical losses [3].

Because the voltage levels are low in a power distribution system, the current magnitude is high and therefore the power losses in the distribution system is of much greater significance in comparison with the transmission system [4]. In order to assure the security standards, the grid must work in an optimal way to properly control the system. That is to reduce the distribution losses and assure the voltage magnitude and the Total Harmonic Distortion (THD) to be within the desired range.

The employment of capacitors was proposed in different studies as a solution. There are different analytical methods to estimate the optimal size and location to install them [5-7]. Most of them consider linear loads, while the ones who dealt with non-linear loads [7, 8] did not take into account the optimum size and dispatch strategy. In spite of their price, which is low in comparison with other var compensators, they are not able to confront the problem of harmonics.

On the other hand, Distribution Static VAR Compensators (D-SVCs) are another convenient way to handle the previous problems, as they have several benefits such as voltage support, power factor correction, loss reduction and billing charge reduction. However, their main advantage lies on the reactive power control and their capacity to mitigate harmonics [9]. It is then required to find an optimal approach to install them with a proper size, in the most convenient locations and to control their dispatch strategy to maximize the savings and assure the grid quality.

Several studies do not offer an integration in their problem formulation to tackle the optimized design of D-SVCs. That is, [10] only studies the location for var compensators without considering their optimum size and operation; the same issue goes for [11, 12] with the difference that they offer an algorithm with a better speed of convergence; [13] integrates the D-SVC's size, however, their optimum operation is still not being considered and authors in [14] give an approach in order to minimize the power losses without bearing in mind economical features. Most of the studies just consider linear loads while the ones who deal with non-linear loads [15, 16] do not take into account the optimum size and dispatch strategy.

Focusing in the optimization techniques, recent investigations present new approaches that are effective in robustness and bring a fast convergence to obtain the solution For instance, [17] implemented an intersect mutation differential evolution method to determine the optimal location and the size of DGs and capacitors simultaneously; the authors in [18] employed a hybrid harmony search algorithm approach in order to minimize power losses in radial distribution networks by determining optimal locations, optimally sized DGs and shunt capacitors; in [19] the optimal allocation for the SVC and DGs has been done using three different indices, namely, Voltage Profile Improvement Index (VPII), Line Loss Reduction Index (LLRI) and Revamp Voltage Stability Indicator (RVSI); [20] proposed an application of Cuckoo search algorithm to determine optimal location and sizing of SVC. Nevertheless, a deeper analysis on them reveals that the optimization for the operational scheduling of the var compensator was not considered or was performed for only a single hour. This is a deficiency on these studies, since load demand is expected to change in time (e.g. peak times, minimal load, among others).

This paper proposes an analytical method which deals with non-linear loads in a radial network and assures power grid quality (related to grid voltage and THD content). This approach allows reducing the conductor's investment and energy losses that are presented in each segment of the feeder, which can be considered as savings. Mathematical models were used for the implementation of the methodology that employs a multi-state Particle Swarm Optimization (PSO) algorithm, at first to select the placement and then to size and next to specify the dispatch strategy of the D-SVCs. Their objectives are to maximize the total savings of the radial power distribution system during a year, subject to voltage and THD standards regulations. The main contribution of this research is that it offers a comprehensive problem formulation to tackle the optimization for sizing, placement and scheduling of D-SVCs, which considers a yearly demand for non-linear loads. The paper continues as follows: section 2 provides the mathematical model for D-SVC, non-linear loads and cost savings; section 3 details the problem formulation in which the objective function and the constraints are described in detail; section 4 gives a description of the proposed methodology, which optimizes the placement, size and yearly dispatch strategy for the D-SVCs by using two stage Particle Swarm Optimization (PSO) algorithms; Three case studies are introduced in section 5; the results are presented and analyzed in section 6; finally, in section 7 the conclusions are provided.

2. Mathematical model

2.1. Distribution Static Var Compensator (D-SVC)

In power systems, the D-SVCs are employed very often due to its versatile and dynamic responses at the need of reactive power demand. They incorporate thyristor controlled reactors (TCR) and thyristor switched capacitor (TSC) for the reactive compensation. The equivalent circuit is introduced in reference [21] and the model is presented in Fig. 1 (a). The mathematical model for the SVC current, is as follows [22]:

$$\overline{I_S} = j\overline{U_M}\left(B_L \frac{2\sigma - \sin(2\sigma)}{\pi} + B_C \right); \sigma = \pi - \alpha \qquad (1)$$

where $\overline{U_M}$ is the system voltage, B_L is the TCR susceptance, B_C is the capacitor susceptance, α is the firing angle measured from positive going zero crossing of the applied voltage and σ is the conduction angle.

The modeling seems to be complex, however it can be simplified as presented:

$$\overline{I_S} = j\overline{U_M}Y_{D-SVC}(\alpha) \qquad (2)$$

Hence, a simple model diagram of the D-SVC is as shown in Fig. 1 (b).

The D-SVC operation primarily depends on the firing angle, which is controlled by using the reference voltage U_S. This control limits the optimum operation for the maximum cost savings. For instance, in a traditional control system, the reference voltage is usually 1.0 p.u. Based on this value, the D-SVC injects a reactive current in order to keep the bus voltage in a desired value. Nevertheless, the injected reactive current may not lead to a maximum cost savings and a new reference voltage value needs to be set as shown

in Fig. 1 (c). Thus, an optimal scheduling for D-SVC is needed.

(a)

(b)

(c)
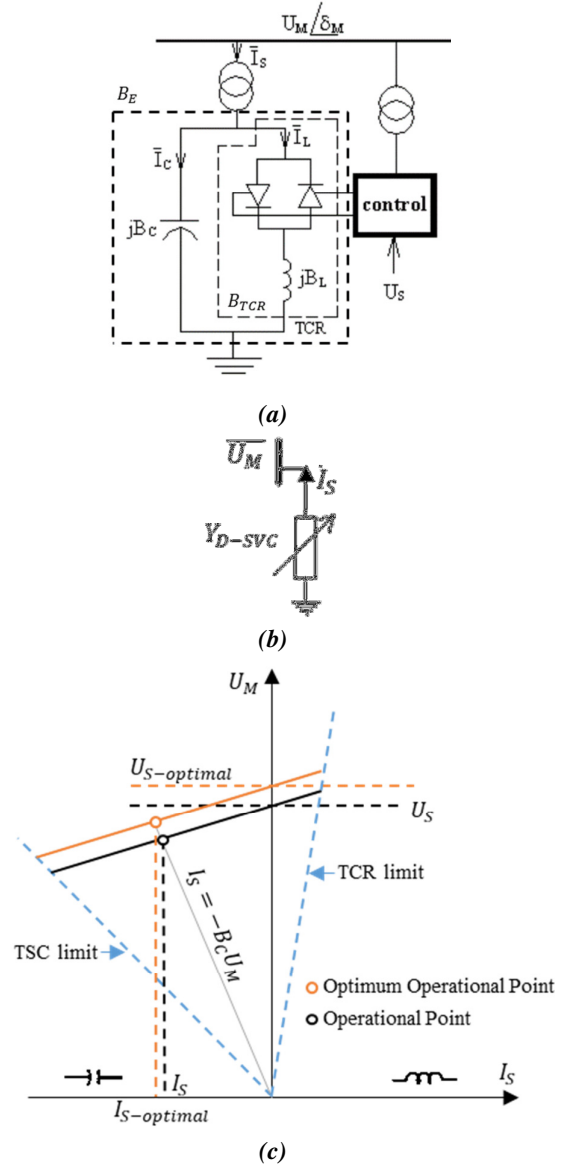
Fig. 1. *D-SVC:* **(a)** equivalent circuit [23]; **(b)** simplify model; **(c)** voltage and current characteristic

2.2. Linear and non-linear loads

Linear loads are the loads that, if supplied by a sinusoidal voltage at the fundamental frequency, produce only the fundamental sinusoidal current [24]. Non-linear loads are the ones that cause distortion in the waveforms of voltage and/or current. These distortions are reflected by the presence of harmonic components in the voltage and current waves.

Non-linear loads are modelled as a RLC load with a current source in parallel [24]. They act as sources of harmonic currents and they circulate current from the load to the source. Depending on the location of these loads in the grid, the harmonic current can spread to other loads. Based on its magnitude, the current injected by the non-linear loads could cause voltage spikes, damage to nearby equipment and can even affect the power supply [25].

2

The THD is useful to express the harmonics content involved in a certain waveform. For instance, the harmonic current component I_h can be written in terms of the total current I and THD [26]:

$$I_h = THD\, I \tag{3}$$

When dealing with a linear load, the total current is formed by an active I_A and a reactive component I_X [27]. Nevertheless, in presence of non-linear loads, based on the Power Vector Configuration approach (applied for non-linear loads) [28], the harmonic component is also considered as follows:

$$\overline{I} = I_A\,\hat{\imath} + I_X\,\hat{\jmath} + I_h\,\hat{k} \tag{4}$$

where $\hat{\imath}$ represent the active power domain, $\hat{\jmath}$ is the reactive power domain and $\hat{k}$ is the harmonics power domain.

Then the apparent current magnitude is:

$$I^2 = I_A^2 + I_X^2 + I_h^2 \tag{5}$$

By replacing (3) into (5) and solving for I:

$$I = \sqrt{\frac{I_A^2 + I_X^2}{1 - THD^2}} \tag{6}$$

The equations defined in this sub-section will be employed for the determination of the cost savings.

2.3. Conductor's investment cost savings estimation

At a planning stage for the installation of a grid, the conductors that are used depend on the electrical conditions. As for example, if high current needs to be transported, thicker and more expensive conductors are required. By employing D-SVCs, the total current flowing from the feeder through the grid could be reduced. The cost savings resulting from this action are referred in this paper as the "conductor's investment cost savings".

Fig. 2 (a) shows a three phase power distribution system for the estimation of cost savings, where P_k is the active power demand, Q_k is the reactive power demand for the kth node and THD_k is the THD of the current for the kth branch that depends on time t, due to load demand variation.

The first scenario is assuming that no D-SVCs are installed, where the three phase active power losses P_L (assuming a balanced system) from segment k of the distribution line is given by:

$$P_{Lk}(t) = 3r_k I_k^2(t) \tag{7}$$
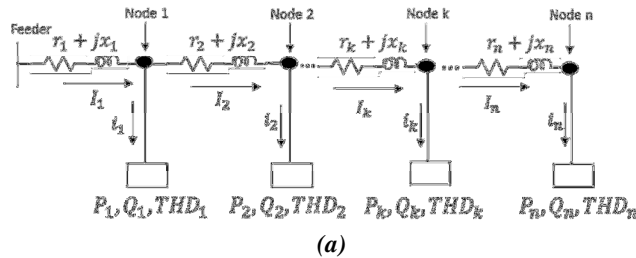
where r_k is the resistance of the segment k and I_k is the magnitude of the downstream apparent current of the radial network. Recalling (6), the magnitude current I_k is:

$$I_k(t) = \sqrt{\frac{I_{Ak}^2(t) + I_{Xk}^2(t)}{1 - THD_k^2(t)}} \tag{8}$$

Hence:

$$P_{Lk}(t) = 3r_k \left(\frac{I_{Ak}^2(t) + I_{Xk}^2(t)}{1 - THD_k^2(t)} \right) \tag{9}$$

A point of interest, is that I_k can be expressed in terms of the real current, reactive current and harmonic current defined by each load upstream (that is from node k to n). The analysis starts from Fig. 2 (a), in which I_k can be written as:

$$\overline{I_k}(t) = \overline{i_k}(t) + \overline{i_{k+1}}(t) + \overline{i_{k+2}}(t) + \text{L} + \overline{i_n}(t)$$

$$\overline{I_k}(t) = \left(\sum_{p=k}^{n} i_{Ap}(t) \right)\hat{\imath} + \left(\sum_{p=k}^{n} i_{Xp}(t) \right)\hat{\jmath} + \left(\sum_{p=k}^{n} i_{hp}(t) \right)\hat{k} \tag{10}$$

Then its magnitude is:

$$I_k^2(t) = \left(\sum_{p=k}^{n} i_{Ap}(t) \right)^2 + \left(\sum_{p=k}^{n} i_{Xp}(t) \right)^2 + \left(\sum_{p=k}^{n} i_{hp}(t) \right)^2 \tag{11}$$

Recalling (3):

$$I_k^2(t) = \left(\sum_{p=k}^{n} i_{Ap}(t) \right)^2 + \left(\sum_{p=k}^{n} i_{Xp}(t) \right)^2 + \left(\sum_{p=k}^{n} i_p(t)THD_p(t) \right)^2 \tag{12}$$

From (5), it is possible to define:

$$I_{Ak}(t) = \sum_{p=k}^{n} i_{Ap}(t) \tag{13}$$

$$I_{Xk}(t) = \sum_{p=k}^{n} i_{Xp}(t) \tag{14}$$

$$I_{hk}(t) = \sum_{p=k}^{n} i_p(t)THD_p(t) \tag{15}$$

Recalling (6), the magnitude i_p must have the form:

$$i_p(t) = \sqrt{\frac{i_{Ap}^2(t) + i_{Xp}^2(t)}{1 - THD_p^2(t)}} \tag{16}$$

Since I_{Ak} and I_{Xk} are known, the challenge is to determine the THD_k as a function of the currents and THD demanded by each load upstream. From (3) it is known that:

$$I_{hk}^2(t) = I_k^2(t)THD_k^2(t) \tag{17}$$

Then (15) can be expressed as:

$$I_k^2(t)THD_k^2(t) = \left(\sum_{p=k}^{n} i_p(t)THD_p(t) \right)^2 \tag{18}$$
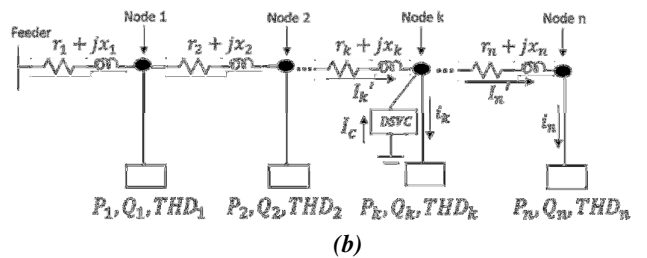

Fig. 2. *Distribution system with non-linear loads: (a) No D-SVC installed; (b) D-SVC installed*

Replacing (8) and (16) in (18) and solving for THD_k:

$$THD_k(t) = \frac{\left(\sum_{p=k}^{n} \sqrt{\frac{i_{Ap}^2(t) + i_{Xp}^2(t)}{1 - THD_p^2(t)}} THD_p(t) \right)}{\sqrt{I_{Ak}^2(t) + I_{Xk}^2(t) + \left(\sum_{p=k}^{n} \sqrt{\frac{i_{Ap}^2(t) + i_{Xp}^2(t)}{1 - THD_p^2(t)}} THD_p(t) \right)^2}} \quad (19)$$

Replacing (13) and (14) in (19)

$$THD_k(t) = \frac{\left(\sum_{p=k}^{n} \sqrt{\frac{i_{Ap}^2(t) + i_{Xp}^2(t)}{1 - THD_p^2(t)}} THD_p(t) \right)}{\sqrt{\left(\sum_{p=k}^{n} i_{Ap}(t) \right)^2 + \left(\sum_{p=k}^{n} i_{Xp}(t) \right)^2 + \left(\sum_{p=k}^{n} \sqrt{\frac{i_{Ap}^2(t) + i_{Xp}^2(t)}{1 - THD_p^2(t)}} THD_p(t) \right)^2}} \quad (20)$$

On the other hand, if a D-SVC is placed at node k, as shown in Fig. 2 (b), it will produce a current I_C that flows to node k. As a result, the current $\overline{I_k}'(t)$ can be expressed as:

$$\overline{I_k}'(t) = \overline{i_k}(t) + \overline{i_{k+1}}(t) + \overline{i_{k+2}}(t) + \text{L} + \overline{i_n}(t) - \overline{I_C} \quad (21)$$

Since the capacitor just produce reactive current then:

$$\overline{I_k}'(t) = \left(\sum_{p=k}^{n} i_{Ap}(t) \right) \vec{S} + \left(\sum_{p=k}^{n} i_{Xp}(t) - I_C \right) \vec{J} + \left(\sum_{p=k}^{n} i_{hp}(t) \right) \vec{k} \quad (22)$$

Recalling (6), $\overline{I_k}'(t)$ magnitude is:

$$I_k'(t) = \sqrt{\frac{I_{Ak}^2(t) + \left(I_{Xk}(t) - I_C \right)^2}{1 - THD_k^2(t)}} \quad (23)$$

The power consumption in segment k of the line with the D-SVC installed can be expressed as:

$$P_{Lk}'(t) = 3r_k \left(I_k'(t) \right)^2 = 3r_k \left(\frac{I_{Ak}^2(t) + \left(I_{Xk}(t) - I_C \right)^2}{1 - THD_k^2(t)} \right)$$

$$P_{Lk}'(t) = 3r_k \left(\frac{I_{Ak}^2(t)}{1 - THD_k^2(t)} + \frac{I_{Xk}^2(t) - 2I_{Xk}(t)I_C + I_C^2}{1 - THD_k^2(t)} \right) \quad (24)$$

$$P_{Lk}'(t) = 3r_k \left(\frac{I_{Ak}^2(t) + I_{Xk}^2(t)}{1 - THD_k^2(t)} + \frac{I_C^2 - 2I_{Xk}(t)I_C}{1 - THD_k^2(t)} \right)$$

When no D-SVC is installed, the conductor on the grid to be installed at segment k is decided based on the maximum P_{Lk}, to assure that the conductor will resist for the worst-case scenario (when the current is the highest). However, when the D-SVC is installed at the node k, the employed conductor for segment k is decided based on the maximum P'_{Lk}, (again, to cover the worst-case scenario). As a result, to find the power losses reduction for segment k called as ΔL_k, the following expression is applied:

$$\Delta L_k = \max \left(P_{Lk}(t) \right) - \max \left(P_{Lk}' \right)$$

$$\Delta L_k = 3r_k I_C \max \left(\frac{2I_{Xk}(t) - I_C}{1 - THD_k^2(t)} \right) \quad (25)$$

Because the D-SVC installed at node k has the potential to reduce the power consumption not only at segment k but also to all other segments, the total reduction of power losses along the system can be rewritten as:

$$\Delta L = \Delta L_1 + \Delta L_2 + \text{L} + \Delta L_n =$$

$$3r_1 I_C \max \left(\frac{2I_{X1}(t) - I_C}{1 - THD_1^2(t)} \right) +$$

$$3r_2 I_C \max \left(\frac{2I_{X2}(t) - I_C}{1 - THD_2^2(t)} \right) + \text{L} \quad (26)$$

$$+ 3r_n I_C \max \left(\frac{2I_{Xn}(t) - I_C}{1 - THD_n^2(t)} \right)$$

The same analysis can be applied for m number of D-SVC ($m \leq n$) located at m different nodes $C_1, C_2, \ldots, C_m$ in ascending order $C_1 < C_2 < \cdots, < C_m$, respectively. By applying the superposition principle, the expression for the total power losses reduction for this scenario is the same as (26) with the only difference that I_C is replaced by $I_C^\dagger$, defined as:

$$I_C^\dagger(t) = \begin{cases} \sum_{q=1}^{m} I_{Cq}(t), & \text{for segment } k \text{ before node } C_1 \\ \sum_{q=2}^{m} I_{Cq}(t), & \text{for segment } k \text{ between nodes } C_1 \& C_2 \\ \quad \text{M} \\ \sum_{q=m}^{m} I_{Cq}(t), & \text{for segment } k \text{ between nodes } C_{m-1} \& C_m \end{cases} \quad (27)$$

where I_{Cq} is the injected current by the D-SVC located at node q.

The savings can be obtained by multiplying the total reduction of power losses by a constant K_L (\$/kW) [29], which represents the savings for using cheaper conductors on the grid:

$$savings_L = K_L \Delta L \quad (28)$$

2.4. Energy savings estimation

These savings are based on the reduction of the energy generated by the bulk supply point due to the presence of D-SVC.

By first considering the scenario in which no D-SVC is installed, the total energy losses at segment k of the grid, during a period T, is given by (29). Note that for this analysis, discretized time is considered.

$$E_{Lk}(t) = \sum_{t=0}^{T} P_{LK}(t) \Delta t \quad (29)$$

By substituting (9) in (29):

$$E_{Lk}(t) = 3r_k \sum_{t=0}^{T} \left(\left(\frac{I_{Ak}^2(t) + I_{Xk}^2(t)}{1 - THD_k^2(t)} \right) \Delta t \right) \quad (30)$$

On the other hand, if a D-SVC is placed in the segment k, it will produce a reactive current I_C. Then, the energy losses on the segment k of the line can be calculated using (24):

$$E_{Lk}(t) = \sum_{t=0}^{T} P_{LK}'(t) \Delta t$$

$$E_{Lk}'(t) = 3r_k \sum_{t=0}^{T} \left(\left(\frac{I_{Ak}^2(t) + I_{Xk}^2(t)}{1 - THD_k^2(t)} + \frac{I_C^2 - 2I_{Xk}(t)I_C}{1 - THD_k^2(t)} \right) \Delta t \right) \quad (31)$$

Hence, the subtraction between (30) and (31) defines the reduction of energy losses for segment k:

4

$$\Delta E_k(t) = E_{Lk}(t) - E_{Lk}{'}(t)$$

$$\Delta E_k(t) = 3r_k I_C \sum_{t=0}^{T} \left(\left(\frac{2I_{Xk}(t) - I_C}{1 - THD_k^{\,2}(t)} \right) \Delta t \right) \qquad (32)$$

The installed D-SVCs at node k will not only reduce the energy losses at segment k, but will also do it for all the line segments. The total reduction of energy losses of the system due to the D-SVC installed at node k can be expressed as:

$$\Delta E(t) = \Delta E_1(t) + \Delta E_2(t) + ... + \Delta E_k(t) =$$

$$3r_1 I_C \sum_{t=0}^{T} \left(\left(\frac{2I_{X1}(t) - I_C}{1 - THD_1^{\,2}(t)} \right) \Delta t \right) +$$

$$3r_2 I_C \sum_{t=0}^{T} \left(\left(\frac{2I_{X2}(t) - I_C}{1 - THD_2^{\,2}(t)} \right) \Delta t \right) + ... \qquad (33)$$

$$+ 3r_n I_C \sum_{t=0}^{T} \left(\left(\frac{2I_{Xn}(t) - I_C}{1 - THD_n^{\,2}(t)} \right) \Delta t \right)$$

In the case that more than one D-SVC is employed, (33) can be adapted by replacing I_C with $I_C^{\dagger}$, given in (27).

The energy savings are calculated by multiplying the reduction of energy losses into a constant K_E [$/kWh] [29], which represents the energy cost:

$$savings_E = K_E \, \Delta E(t) \qquad (34)$$

2.5. Cost D-SVC estimation

This cost is due to the expenses required to acquire the D-SVCs. For simplicity, a linear relation is assumed between the capacity Q_{DSVC} and a constant K_{DSVC} [$/kVAR]:

$$COST_{DSVC} = K_{DSVC} \, Q_{DSVC} \, ceil\left(\frac{T}{T_{DSVC}} \right) \qquad (35)$$

where T_{DSVC} is the lifetime of the D-SVC and *ceil* is a function which rounds its argument up to the next integer. The *ceil* function is required in case the lifetime of the D-SVC is lower than the one in the system. This means that a new D-SVC must be installed when the previous one has reached its lifetime.

2.6. Total savings estimation

Finally, the total savings for the system T_S [$] is given by:

$$T_S = K_L \Delta L + K_E \Delta E - K_{DSVC} Q_{DSVC} \qquad (36)$$

3. Problem formulation

The main objective of this paper is to minimize the total power distribution losses and hence get the maximum value for the economic savings (which is considered as the objective function), subject to the constraints of the system.

An hourly time-slotted system with slot index t is considered for this formulation. The optimization problem can be defined as:

$$maximize \left(\sum_{i=1}^{n} savings_P(i) + \sum_{t=1}^{T} \sum_{i=1}^{n} savings_E(i,t) - \sum_{i=1}^{n} cost_{DSVC}(i) \right) \qquad (37)$$

Subject to:

$$P_{grid}(t) - \sum_{i=1}^{n} P_{losses}(i,t) = \sum_{i=1}^{n} P_{load}(i,t), \, j = 1, 2, ..., n$$
$$, \, t = 1, 2, ..., T \qquad (38)$$

$$Q_{grid}(t) + \sum_{i=1}^{n} Q_{DSVC}(i,t) - \sum_{i=1}^{n} Q_{losses}(i,t) = \sum_{i=1}^{n} Q_{load}(i,t),$$
$$i = 1, 2, ..., n; \, t = 1, 2, ..., T \qquad (39)$$

$$Q_{\min}(i) \le Q_{DSVC}(i,t) \le Q_{\max}(i), i = 1, 2, ..., n; \, t = 1, 2, ..., T \qquad (40)$$

$$V_{p.u.\min} \le |V_{p.u.}(i,t)| \le V_{p.u.\max}, \, i = 1, 2, ..., n; \, t = 1, 2, ..., T \qquad (41)$$

$$0 \le THD_V(i,t) \le THD_{V\_\max}, \, i = 1, 2, ..., n; \, t = 1, 2, ..., T \qquad (42)$$

$$0 \le m \le n \qquad (43)$$

where i represents the node number and n is the total number of nodes.

The constraints shown in (38) and (39) indicate that the power (real or reactive) carried by the feeder should satisfy the load and the electrical power losses. The reactive power produced by an installed D-SVC is constrained by (40), since it has a minimum and maximum defined power. In addition, (41) follows the IEEE Standard 1860-2014 [30] which states that utility distribution nodes should provide a voltage regulation. On the other hand, (42) follows the IEEE Standard 519-2014 [31] which requires that there should be a regulation for the total harmonic distortion. Finally, constraint (43) is employed to control the number m of installed D-SVC. Note that only one D-SVC is allowed to be installed per node.

4. Algorithm

The current optimization problem cannot be solved employing basic mathematical methods or exact optimization algorithms because of the power flow analysis which is based on an iterative process. As a result, a meta-heuristic optimization algorithm will be applied. Regardless of the fact that these methods cannot assure to obtain the global solution, they are able to provide a sufficiently good solution.

In the last decade, several studies have been done related with the optimal placement of SVC. These studies used different algorithms such as Particle Swarm Optimization (PSO) [10], Non-Dominated Sorting Particle Swarm Optimization (NDPSO) [11], Global Harmony Search [12, 13], Differential Evolution (DE) [14] and Cuckoo search [32]. Among them, PSO is chosen as the algorithm to be used in this study. This decision is based on the advantages it presents over other optimization algorithms, such as: (1) easy implementation; (2) stronger memorization capability achieved; (3) equal evolution opportunity for all candidate solutions; (4) low computer memory requirement; (5) descent convergence speed due to only primitive mathematical operators [33, 34].

PSO defines an initial population of particles, each of them is at a particular position $x_p(h)$ with a given operational point. These are then evaluated on the system in order to select the best global particle position $g(h)$ and best

individual particle position $\hat{x}_p(h)$ for the current iteration h, which are used to calculate the speed of each particle $v_p(h+1)$ for the next iteration $h+1$, as shown:

$$v_p(h+1) = \omega v_p(h) + c_1 r_1 \left(\hat{x}_p(h) - x_p(h) \right) + c_2 r_2 \left(g(h) - x_p(h) \right) \quad (44)$$

where p is the index of the particle, r_1 and r_2 are random numbers uniformly distributed between [0,1]. The parameters ω, c_1, c_2 are weightings for inertia such that $0 \leq \omega \leq 1.2$, $0 \leq c_1, c_2 \leq 2$. Based on an empirical analysis, ω, c_1 and c_2 values were chosen 0.2, 0.4 and 0.4 respectively.

Based on (44), the particle position for the next iteration is:

$$x_p(h+1) = x_p(h) + v_p(h+1) \quad (45)$$

On the other hand, this paper focus on the optimisation of D-SVC size, which refers to the best capacity of the D-SVC that maximizes the cost savings. While Dispatch strategy refers to the control of the power output of the already installed D-SVC. A significant advantage of D-SVCs in comparison with capacitors is that they can vary its var compensation and here comes the novelty of the proposed approach. The employed optimization technique is called Multi Particle Swarm Optimization, because it implements a PSO within another PSO. Consequently, this approach is convenient to assure an optimum D-SVC's operation. An external PSO called PSO_{si}, is used to estimate the optimal placement and size for the D-SVC, while the second is an internal one called PSO_{ds} that allows to get their optimal dispatch strategy.

The process starts by defining the input data of the system such as line voltage, daily power consumption, total harmonic distortion for the load, line impedances and available D-SVCs in stock. Next, the maximum number of iterations for PSO_{si} and PSO_{ds} are defined. For PSO_{si}, an initial population of particles is randomly generated. Each particle is a possible solution for the objective function, therefore, each of these become a set of var compensators with a given size and placement (the placement is defined by a setting the D-SVC at a node of the system). Initially, the particles are chosen randomly (random in number, size, and placement), then a new set of particles (here starts PSO_{ds}) is defined. This new particle takes a value of operation between the maximum and minimum reactive power given by the set of particles previously generated. Later, to estimate the currents and voltages on the grid, a power flow calculation based on the Backward/Forward Sweep Load Flow method is performed. Consequently, the total savings for each particle are obtained using (36). The particle with the best solution becomes the global best. Then, each particle starts moving (change its operation point) based on the best global by using (44) and (45). If there is a particle that achieves an improved total saving, the global best is updated and the particle with this solution becomes the new global best. A point to consider is the local best, which is the best result before and after particle's movement. Then, PSO_{si} particles are compared to obtain the best result and the set with the optimum number, size and placement of D-SVC is obtained. This process is repeated until the maximum number of iterations has been reached or if the values of the savings have a difference of 10^{-6} between the current and previous iteration, assuring a convergence in the solution. At the end of the simulation the best solution from the PSO_{si} (placement and size) with its respective value of the optimization parameters from the PSO_{ds} (dispatch strategy optimization) are obtained.
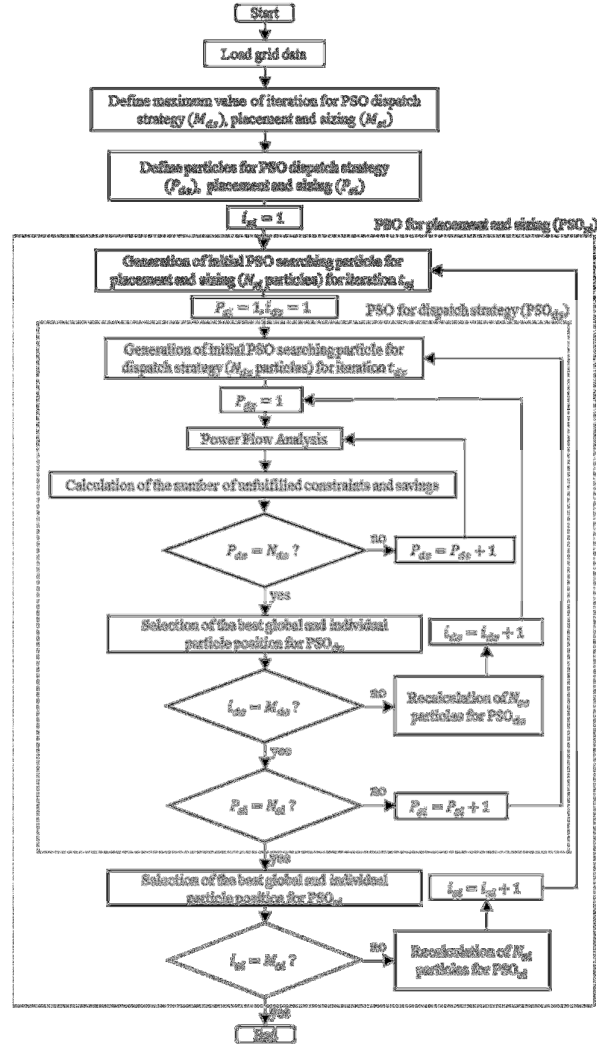

Fig. 3. *Proposed Multi particle Swarm Optimization flowchart*

By this approach, the optimal placement, size and dispatch strategy of the D-SVCs in the grid are selected by solving the optimization problem described in section IV. Fig. 3 shows the proposed algorithm in a flowchart form which was implemented in Matlab.

5. Case Study

In order to show the efficacy of the proposed algorithm considering the proposed mathematical formulations given in the paper, the following case is studied. The studied systems are three IEEE distribution systems: (1) 9 bus [35]; (2) 69 bus [36]; (3) 119 bus [37]. It is then required to maximize the savings associated to the grid power losses ΔL and energy consumption ΔE by adding reactive power compensators. A total of three scenarios are evaluated: 1. no VAR compensators are installed; 2. only capacitors are used; 3. only D-SVCs are installed. To simplify the analysis, the assumptions are as follows: 1. load balanced conditions; 2. negligible line capacitance; 3. time-

6

variant loads; 4. time-variant harmonic generation at each point of the node; 5. the yearly load demand profile is kept constant; 6. conductor data is taken from [35-38]. 7. Ssame number of capacitors and D-SVCs are available.
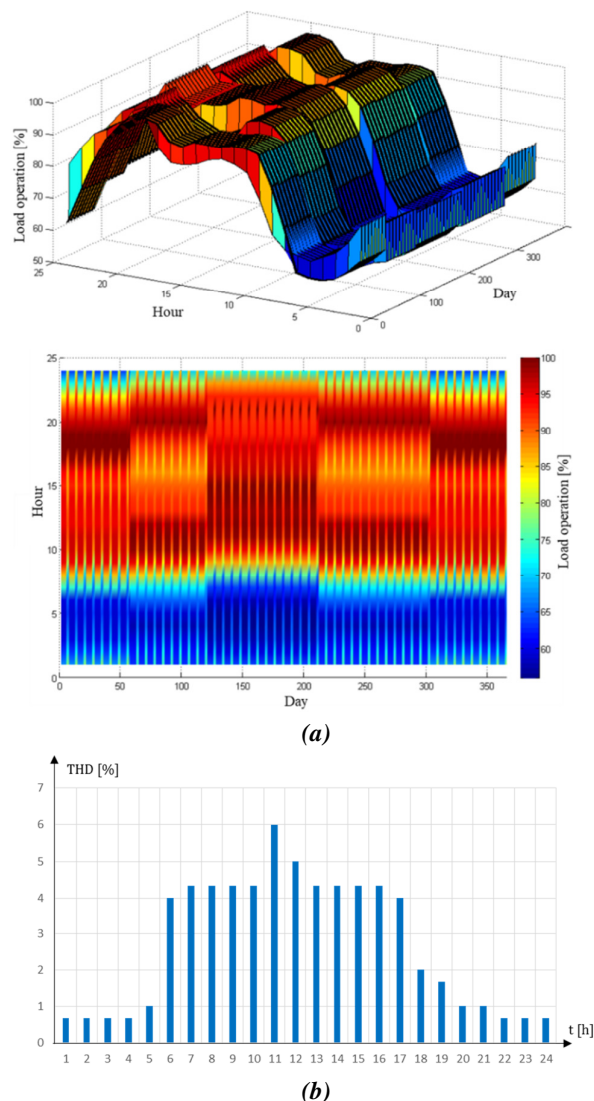

(a)

(b)

Fig. 4. *System data:* **(a)** Yearly load profile; **(b)** 24-hours Total Harmonic Distortion

The yearly normalized load demand employed for the current investigation is presented in Fig. 4 (a). The load demand of each node is obtained by multiplying the previous load profile into each of the P & Q values defined for each node according to the respective IEEE bus system. In addition, the 24 hours THD profile for a single load is assumed as shown in Fig. 4 (b). For simplicity, it is considered to be the same every day for all the loads and all the IEEE distribution systems. All data related with the available capacitors, D-SVCs and constants are assumed as shown in Table 1.

The grid has some regulations that must met. Following the IEEE Standard 1860-2014 [18], utility distribution nodes should provide a voltage between 0.95 p.u. and 1.05 p.u. In addition, according to the IEEE

Standard 519-2014 [19], utility distribution nodes should provide a harmonic distortion level of less than 5% provided customers on the distribution feeder limit their load harmonic current injections to a prescribed level.

Table 1. VAR Components Specifications

Available 3-phase D-SVC		
kVAR$_{max}$	1000	2000	3000
Available 3-phase fixed capacitors		
kVAR	1000	2000	3000
Constants		
K_L	K_{DSVC}	K_C	K_E
168 [\$/kW]	10.0 [\$/kVAR]	4.00 [\$/kVAR]	0.08 [\$/kWh]

6. Results and discussion

The results were obtained through the proposed algorithm, which was run using a computer with a RAM of 8.00 GB and processor Intel Core i7-6700 of 3.40 GHz. The optimization algorithm was run 10 times for each case study. The robustness of our approach is appreciated as the highest difference between the best and worst result with values of 5.3%, 7.6% and 8.6% for the case study of 9 Bus IEEE, 69 Bus IEEE and 119 bus IEEE, respectively. Furthermore, the average simulation time to perform the scheduling optimization for each time slot were 0.19 seconds, 0.31 seconds and 0.76 seconds for the case study of 9 Bus IEEE, 69 Bus IEEE and 188 bus IEEE, respectively.

In order to get the voltage and THD profiles at each node, a power flow analysis using the Backward/Forward Sweep Load Flow method was run for each IEEE distribution system. Among the different power flow methods, the current one was chosen due to its accurate and fast convergence when dealing with radial distribution systems [39] assuring by this the implementation of the dispatch strategy in real life. As a result, a box plot as given in Fig. 5 is obtained. This provides the maximum, minimum, median and percentage of times that the system is within the voltage and THD permitted range, which is calculated as follows:

$$\% range = \frac{\sum_{i=1}^{n_{max}} \sum_{j=1}^{T} x_{i,j}}{n_{max} T} \times 100\% ; x_{i,j} = \begin{cases} 1, if\ x_{i,j}\ within\ the\ range \\ 0, if\ x_{i,j}\ outside\ the\ range \end{cases} \quad (46)$$

where n_{max} is the maximum number of nodes.

Case 1: Non-VAR Compensator Installed

Initially, the voltage and THD for all the systems at some nodes are not in the desired range $(0.95\ p.u. \le V \le 1.05\ p.u\ \&\_THD \le 5\%)$, as shown in Table II (case 1). Moreover, the percentage of times that the voltage and THD meet the regulations is no more than 50% and 80% respectively. This scenario is employed as the benchmark to analyse the performance of the others.

6.1. Case 2: Capacitors are installed

The optimum number of installed capacitors for each test system is shown in Table 2. The savings in this scenario are obtained by the installation of capacitors. An operational scheduling for fixed capacitors is redundant since the

reactive current that they can give is constant. However, there is an optimal size and placement for capacitors. As a result, only the PSO_{si} algorithm is employed. Their optimum size and placement for each IEEE distribution system is presented in Fig. 6 (a).

With the implementations of the capacitors, the maximum and minimum voltage for all the systems reaches values close to the limits, showing an improvement in their average values. The voltage profile shows an enhancement in the system since the percentage of times is within the allowed range is greater than 85% for all IEEE systems as shown in Fig. 5 (a) and Table 3. Nevertheless, for the THD profile, it presents an increment in comparison to case one as presented in Fig. 5 (b) and Table 4.
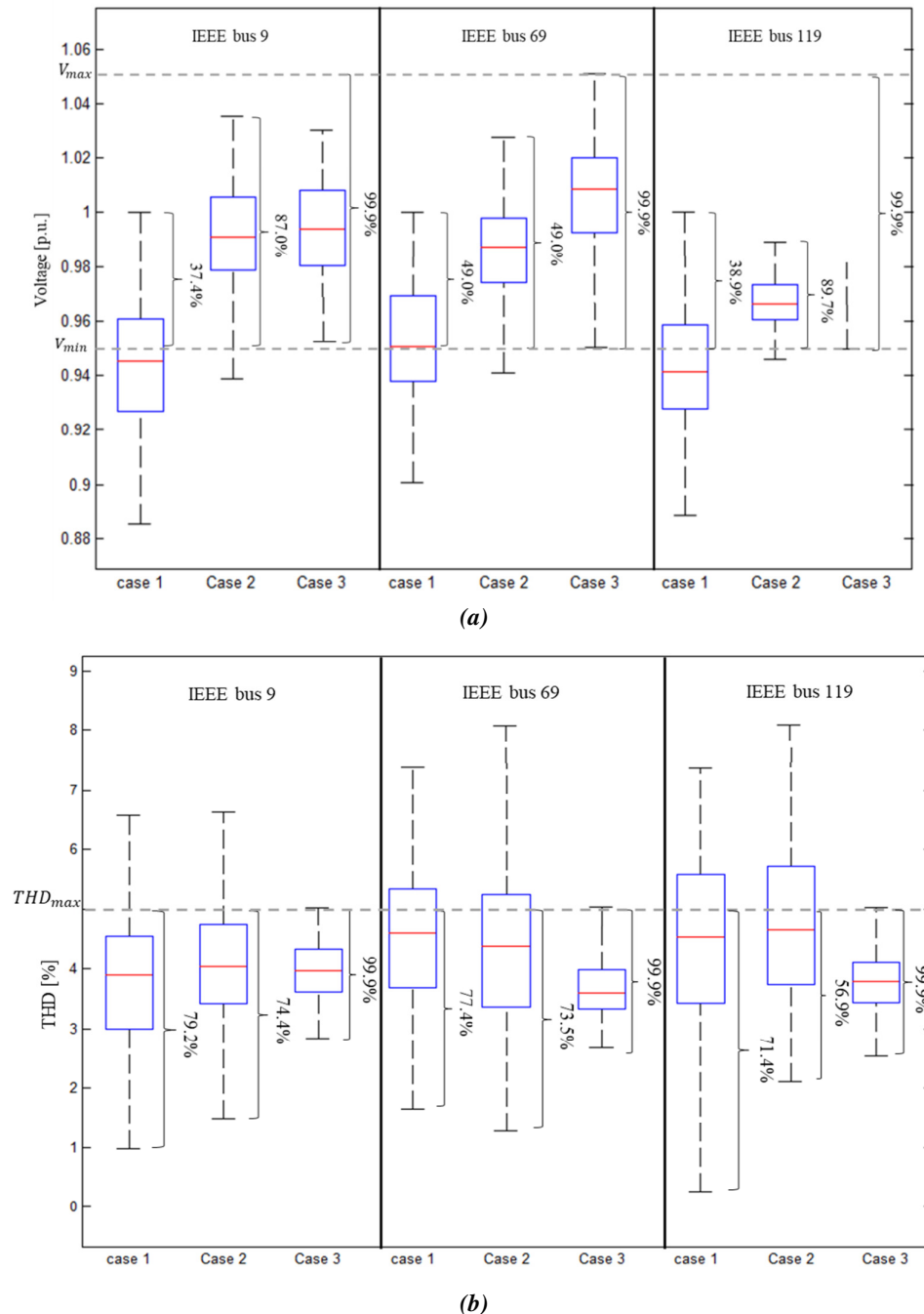

(a)

(b)

Fig. 5. *Summary:* **(a)** voltage profile; **(b)** THD profile

Table 2. Optimum number of var compensators installed

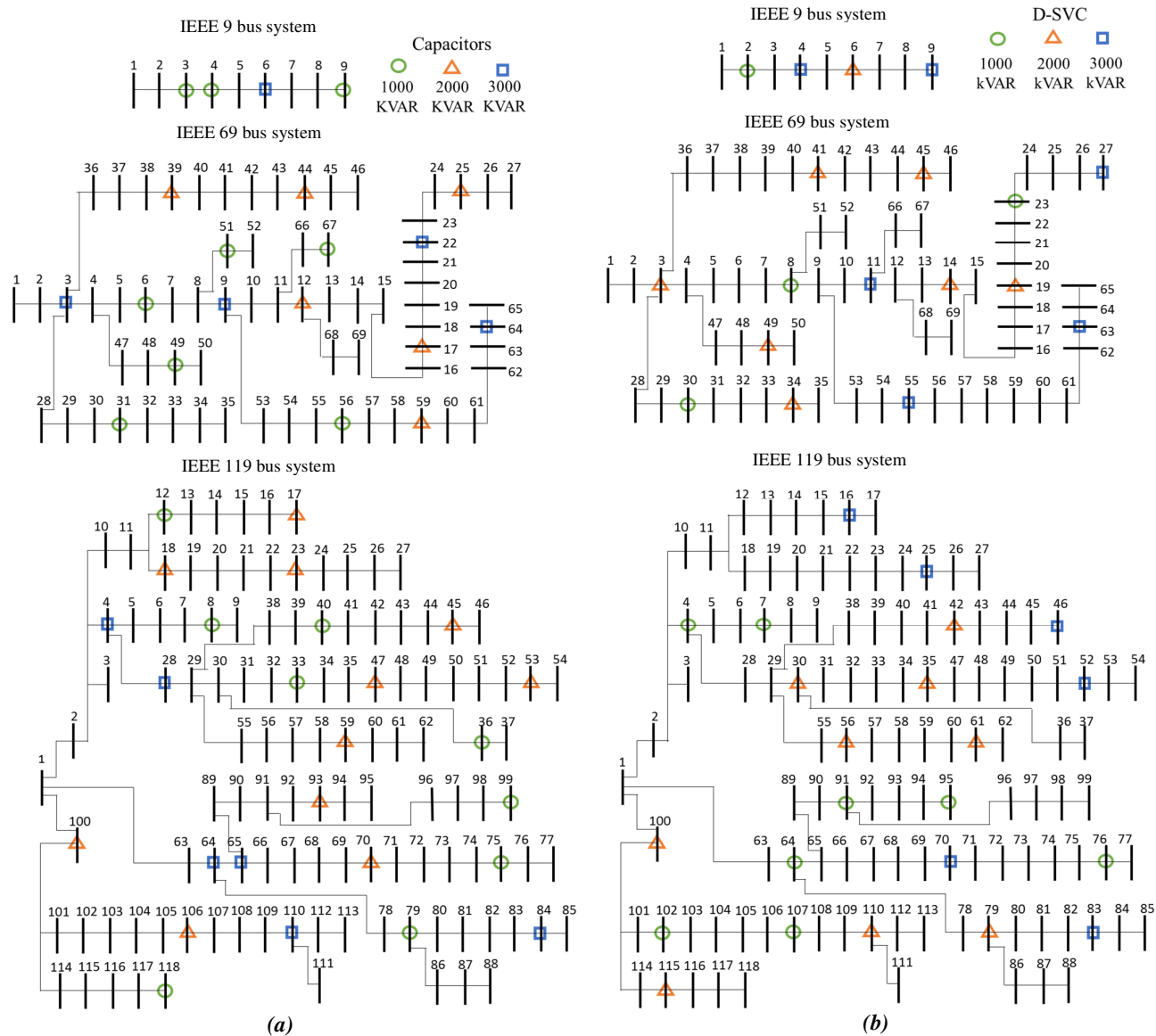| Total number of	IEEE 9	IEEE 69	IEEE 119
Capacitors installed	4	15	27
D-SVCs installed	4	14	23

8

Fig. 6 *Optimum size and placement for:* **(a)** Capacitor; **(b)** D-SVC

Table 3. Capacitors' optimum size and placement

Capacitor size [kVAR]	IEEE 9 capacitor installed at node	IEEE 69 capacitor installed at node	IEEE 119 capacitor installed at node
1000	3, 4, 9	6, 31, 49, 51, 56, 67	8, 12, 33, 36, 40, 36, 75, 79, 99, 118
2000	none	12,17, 25, 39, 44	17, 18, 23, 45, 47 53, 59, 93, 70, 100, 106
3000	6	3, 9, 22, 64	4, 28, 64, 65, 84, 110

Table 4. D-SVCs' optimum size and placement

Capacitor size [kVAR]	IEEE 9 D-SVC installed at node	IEEE 69 D-SVC installed at node	IEEE 119 D-SVC installed at node
1000	2	8, 23, 30	4, 7, 64, 76, 91, 95, 102, 107
2000	6	3, 14, 19, 34, 41, 45, 59	30, 35, 42, 56, 61, 79, 100, 110, 115
3000	4, 9	11,27, 55, 63	16, 25, 46, 52, 70, 83

6.2. Case 3: D-SVCs are installed

The optimum number of D-SVCs may not be necessarily the same as the optimum number of capacitors. Indeed, the results show that depending on the test system, the optimum number of D-SVC could be equal or less than the number of capacitors, as presented in Table 2. On the other hand, the D-SVCs show a better regulation for voltage and THD for all the distribution systems as given in Fig. 5 (a) and Fig. 5 (b), respectively. Their optimum operation scheduling does not only allow the maximization of savings, it also keeps the voltage in the desire range and reduce the THD. Fig. 6 reveals that the number of capacitors employed for the optimization is greater or equal in comparison with the number of D-SVC. This is due to the flexibility of the D-SVC to inject reactive power. In contrast with the capacitors, the D-SVCs can vary the reactive power that they can feed on, and an operation scheduling is needed to maximize the savings. Hence, the full proposed algorithm is applied. The optimum size and placement of the D-SVCs for each distribution system is presented in Fig. 6 (b) and their optimal operation point for each D-SVC during minimal and peak load demand is shown in **Error! Reference source not found.**.
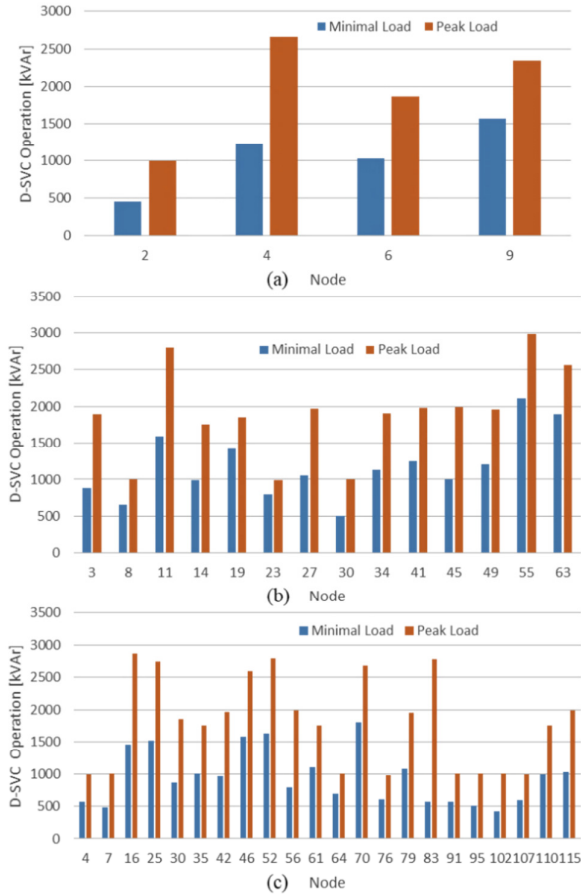
The cost savings depends on the power losses and energy reduction and acquisition cost of the VAR compensators. Fig. 8 gives the accumulated power loss profile and by this the energy savings (i.e. the area under the curve) for the three cases per month. It is notable that with the inclusion of reactive power compensators, the power losses are reduced. For instance, with the installation of capacitors the percentage reduction of power losses are 6.3%, 11% and 13% for the 9 bus, 69 bus and 119 bus, respectively. Nevertheless, the inclusion of D-SVCs have a better power loss reduction than capacitors, since the percentage reduction of power losses are 9.4%, 15% and 22% for the 9 bus, 69 bus and 119 bus, respectively. Hence, the total savings during the first year will be more for the D-SVCs than capacitors as shown in `Table 5`.
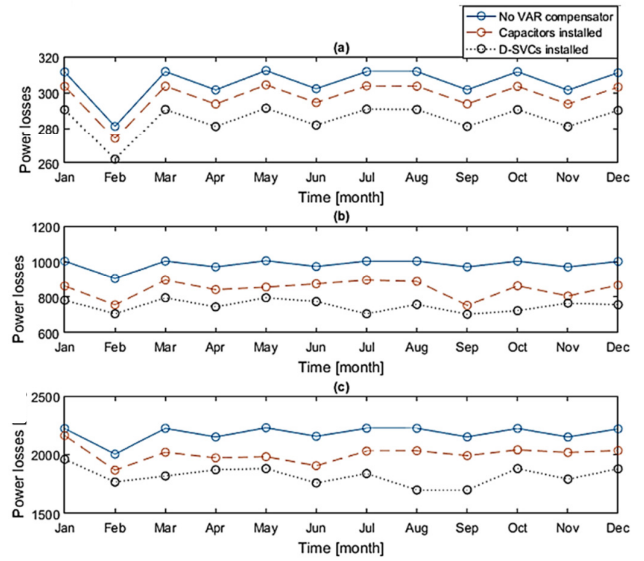

Fig. 8. *Power losses profile [kW]*
(a) 9 bus; **(b)** 69 bus; **(c)** 119 bus

Fig. 7. *Optimal D-SVC operation during minimal and peak load:* **(a)** 9 bus; **(b)** 69 bus; **(c)** 119 bus

Table 5. First Year Cost-Savings Summary

Case 2			
Cost-Savings	IEEE 9	IEEE 69	IEEE 119
Energy savings [$]	13978	87164	175200
Conductor's investment savings [$]	10562	59120	104018
Capacitor cost [$]	12000	120000	196000
Total Savings [$]	12540	26284	83218
Case 3			
Cost-Savings	IEEE 9	IEEE 69	IEEE 119
Energy savings [$]	68032	185200	235360
Conductor's investment savings [$]	65145	146857	253396
D-SVC cost [$]	120000	300000	490000
Total Savings [$]	13177	32057	98756

7. Conclusion

This paper proposes an approach to maximize the cost savings based on the optimization of the placement, size and dispatch strategies of the D-SVCs. The approach incorporates particle swarm optimization algorithms in two-stages, one for the optimization of the placement and size of the D-SVCs and the other for the optimization of their dispatch strategy.

The obtained results with the installation of capacitors and D-SVCs showed a good voltage regulation, following the IEEE Standard 1860-2014. However, only with the installation of D-SVCs, the THD was kept in the desired range meeting the IEEE Standard 519-2014. Despite the fact that the acquisition cost of the D-SVCs is higher than the one of the capacitors, the former ones can adjust their dispatch strategy to maximize the final savings. Hence, the optimization of the system by installing D-SVCs proved to be superior in comparison to the one in which capacitors are installed giving higher savings and better grid quality.

8. Acknowledgments

9. References

[1] A. Caillé, M. Al-Moneef, F. B. de Castro, A. Bundgaard-Jensen, A. Fall, N. F. de Medeiros, *et al.*, "2007 Survey of Energy Resources," *World Energy Council,* vol. 2007, 2007.

[2] M. Yano, S. Abe, and E. Ohno, "History of power electronics for motor drives in Japan," in *IEEE Conference on the History of Electronics*, 2004, pp. 1-11.

[3] F. C. Pereira, O. C. Souto, J. C. De Oliveira, A. L. Vilaça, and P. F. Ribeiro, "An analysis of costs related to the loss of power quality," in *Harmonics and Quality of Power Proceedings, 1998. Proceedings. 8th International Conference On*, 1998, pp. 777-782.

[4] P. P. Barker and R. W. De Mello, "Determining the impact of distributed generation on power systems. I. Radial distribution systems," in *Power Engineering Society Summer Meeting, 2000. IEEE*, 2000, pp. 1645-1656.

[5] Y. M. Shuaib, M. S. Kalavathi, and C. C. A. Rajan, "Optimal capacitor placement in radial distribution system using gravitational search algorithm," *International Journal of Electrical Power & Energy Systems,* vol. 64, pp. 384-397, 2015.

[6] J. Vuletić and M. Todorovski, "Optimal capacitor placement in distorted distribution networks with different load models using Penalty Free Genetic Algorithm," *International Journal of Electrical Power & Energy Systems,* vol. 78, pp. 174-182, 2016.

[7] M. S. Javadi, A. E. Nezhad, P. Siano, M. Shafie-khah, and J. P. Catalão, "Shunt capacitor placement in radial distribution networks considering switching transients decision making approach," *International Journal of Electrical Power & Energy Systems,* vol. 92, pp. 167-180, 2017.

[8] S. Kawasaki and G. Ogasawara, "Influence analyses of harmonics on distribution system in consideration of non-linear loads and estimation of harmonic source," *Journal of International Council on Electrical Engineering,* vol. 7, pp. 76-82, 2017.

[9] M. Noroozian, N. Petersson, B. Thorvaldson, A. Nilsson, and C. Taylor, "Benefits of SVC and STATCOM for electric utility application," in *Transmission and Distribution Conference and Exposition, 2003 IEEE PES*, 2003, pp. 1143-1150.

[10] M. Saravanan, S. M. R. Slochanal, P. Venkatesh, and J. P. S. Abraham, "Application of particle swarm optimization technique for optimal location of FACTS devices considering cost of installation and system loadability," *Electric Power Systems Research,* vol. 77, pp. 276-283, 2007.

[11] R. Benabid, M. Boudour, and M. Abido, "Optimal location and setting of SVC and TCSC devices using non-dominated sorting particle swarm optimization," *Electric Power Systems Research,* vol. 79, pp. 1668-1677, 2009.

[12] R. Sirjani, A. Mohamed, and H. Shareef, "Optimal allocation of shunt Var compensators in power systems using a novel global harmony search algorithm," *International Journal of Electrical Power & Energy Systems,* vol. 43, pp. 562-572, 2012.

[13] R. Sirjani and A. Mohamed, "Improved harmony search algorithm for optimal placement and sizing of static var compensators in power systems," in *Informatics and Computational Intelligence (ICI), 2011 First International Conference on*, 2011, pp. 295-300.

[14] S. Udgir, L. Srivastava, and M. Pandit, "Optimal placement and sizing of SVC for loss minimization and voltage security improvement using differential evolution algorithm," in *Recent Advances and Innovations in Engineering (ICRAIE), 2014*, 2014, pp. 1-6.

[15] M. Abdulla and Z. Salameh, "A graphical method to determine the harmonic magnification in radial feeders due to SVC operation," *Electric Power Systems Research,* vol. 57, pp. 9-14, 2001.

[16] H. L. Wang and M. S. Lin, "A probabilistic approach for SVC placement with harmonic control and reactive power compensation," in *2015 IEEE Innovative Smart Grid Technologies - Asia (ISGT ASIA)*, 2015, pp. 1-6.

[17] A. Khodabakhshian and M. H. Andishgar, "Simultaneous placement and sizing of DGs and shunt capacitors in distribution systems by using IMDE algorithm," *International Journal of Electrical Power & Energy Systems,* vol. 82, pp. 599-607, 2016.

[18] K. Muthukumar and S. Jayalalitha, "Optimal placement and sizing of distributed generators and shunt capacitors for power loss minimization in radial distribution networks using hybrid heuristic search optimization technique," *International Journal of Electrical Power & Energy Systems,* vol. 78, pp. 299-319, 2016.

[19] A. Rath, S. R. Ghatak, and P. Goyal, "Optimal allocation of distributed generation (DGs) and static VAR compensator (SVC) in a power system using Revamp Voltage Stability Indicator," in *Power Systems Conference (NPSC), 2016 National*, 2016, pp. 1-6.

[20] K. P. Nguyen, G. Fujita, and V. N. Dieu, "Cuckoo search algorithm for optimal placement and sizing of static var compensator in large-scale power systems," *Journal of Artificial Intelligence and Soft Computing Research,* vol. 6, pp. 59-68, 2016.

[21] M. Mahdavian, G. Shahgholian, P. Shafaghi, M. Azadeh, S. Farazpey, and M. Janghorbani, "Power system oscillations improvement by using static VAR compensator," in *Electrical Engineering/Electronics, Computer, Telecommunications and Information Technology (ECTI-CON), 2016 13th International Conference on*, 2016, pp. 1-5.

[22] J. Faiz and G. Shahgholian, "Modeling and damping controller design for static var compensator," in *Power Engineering, Energy and Electrical Drives (POWERENG), 2015 IEEE 5th International Conference on*, 2015, pp. 405-409.

[23] I. Pisica, C. Bulac, L. Toma, and M. Eremia, "Optimal SVC placement in electric power systems using a genetic algorithms based method," in *PowerTech, 2009 IEEE Bucharest*, 2009, pp. 1-6.

[24] R. Burch, G.-k. Chang, C. Hatziadoniu, M. Grady, Y. Liu, M. Marz, *et al.*, "Impact of aggregate linear load modeling on harmonic analysis: A comparison of common practice and analytical models," *IEEE Transactions on Power Delivery,* vol. 18, pp. 625-630, 2003.

[25] V. Wagner, J. C. Balda, D. Griffith, A. Mceachern, T. Barnes, D. Hartmann, *et al.*, "Effects of harmonics on equipment," *IEEE Transactions on Power Delivery,* vol. 8, pp. 672-680, 1993.

[26] L. Rozenblat. (2004, A primer on work and ac power in electrical circuit definitions and math equations for watt, VA, power factor and THD. Available: http://www.smps.us/power.html

[27] J. D. Glover, M. S. Sarma, and T. Overbye, *Power System Analysis & Design, SI Version*: Cengage Learning, 2012.

[28] A. Hoevenaars, "How harmonics have contributed to many power factor misconceptions," Mirus International Inc. January 15, 2014.

[29] M. Gheydi and M. J. Golkar, "Optimal capacitor placement in distribution network with consideration of annual load profile: Case study Meshkinshahr distribution network," in *IECON 2016 - 42nd Annual Conference of the IEEE Industrial Electronics Society*, 2016, pp. 7208-7214.

[30] "IEEE Guide for Voltage Regulation and Reactive Power Compensation at 1000 kV AC and Above," *IEEE Std 1860-2014,* pp. 1-41, 2014.

[31] "IEEE Recommended Practice and Requirements for Harmonic Control in Electric Power Systems - Redline," *IEEE Std 519-2014 (Revision of IEEE Std 519-1992) - Redline,* pp. 1-213, 2014.

[32] X.-S. Yang and S. Deb, "Cuckoo search via Lévy flights," in *Nature & Biologically Inspired Computing, 2009. NaBIC 2009. World Congress on*, 2009, pp. 210-214.

[33] C. Shang, D. Srinivasan, and T. Reindl, "An improved particle swarm optimisation algorithm applied to battery sizing for stand-alone hybrid power systems," *International Journal of Electrical Power & Energy Systems,* vol. 74, pp. 104-117, 2016.

[34] A. E. Eiben and J. E. Smith, *Introduction to evolutionary computing* vol. 53: Springer, 2003.

[35] M. M. Hamada, M. A. Wahab, A.-H. M. El-Sayed, and H. A. Ramadan, "A new approach for capacitor allocation in radial distribution feeders," *Online J Electron Electr Eng (OJEEE),* vol. 1, pp. 24-29, 2006.

[36] J. Savier and D. Das, "Impact of network reconfiguration on loss allocation of radial distribution systems," *IEEE Transactions on Power Delivery,* vol. 22, pp. 2473-2480, 2007.

[37] D. Zhang, Z. Fu, and L. Zhang, "An improved TS algorithm for loss-minimum reconfiguration in large-scale distribution systems," *Electric Power Systems Research,* vol. 77, pp. 685-694, 2007.

[38] D. Kaur, J. Sharma " Optimal conductor sizing in radial distribution systems planning," *International Journal of Electrical Power & Energy,* vol. 30(4), pp. 261-271, 2008.

[39] S. Ghosh and D. Das, "Method for load-flow solution of radial distribution networks," *IEE Proceedings-Generation, Transmission and Distribution,* vol. 146, pp. 641-648, 1999.